PHYSICAL REVIEW D VOLUME 18, NUMBER 5 1 SEPTEMBER 1978

High-spin meson decays in the dual resonance model with nondegenerate Regge trajectories

M. Kuroda
Deutsches Elektronen-Synchrotron DESY, Hamburg, Germany

T. F. Walsh
*Sektion Physik, Universität Wuppertal, Wuppertal, Germany and Deutsches Elektronen-Synchrotron DESY, Hamburg, Germany**

Bing-Lin Young
Ames Laboratory ERDA and Department of Physics, Iowa State University, Ames, Iowa, 50010
(Received 2 November 1977; revised manuscript received 13 April 1978)

We discuss the decays of high-spin natural-parity resonances lying on a leading Regge trajectory. We do this by studying the reaction $VP \to PP$ in a dual resonance model with trajectories which are nondegenerate in the resonance region. This allows for SU(4)-symmetry breaking in meson decay rates. Owing to the factorization property of Regge slopes and to the equal-spacing rule, we find rates which depend only on an overall normalization (and the low s ρ trajectory slope α_ρ'). Agreement with data is good.

I. INTRODUCTION

It is well established by now that the nonrelativistic quark model gives a good description of the low-lying quark bound states (including charm). Less clear is how the quark model can describe high-angular-momentum excitations—particularly since these lie on Regge trajectories and appear in amplitudes satisfying duality constraints. The most compact and satisfactory description of these states on leading trajectories is in terms of dual resonance models, or, simpler, via a one-term Veneziano ansatz for the scattering amplitude. In some sense this represents an extreme case of the quark model still not fully accessible through the standard bound-state picture. It is well known that a single-term Veneziano formula cannot be an adequate description of a scattering amplitude. We do believe, however, that the simple Veneziano formulation will survive as a procedure for calculating the couplings of high-L $q\bar{q}$ excitations on the leading Regge trajectories. In particular, it offers a way of incorporating the symmetry-breaking effects of unequal quark (or meson) masses. It is for this purpose that we will employ the Veneziano model.

Experiment requires that we admit Regge trajectories which at low s (in the resonance region) do not have common slopes.[1,2] This means that there is no universal spacing of resonances in (mass)^2. The quark model has no trouble with this, but the same cannot be said of dual resonance models. If trajectory slopes are constant and are not degenerate, a well-known disease occurs (noted by Mandelstam[3]): A scattering amplitudes diverge at large s as $|t|$ increases.

The trouble caused by nondegenerate slopes in the Veneziano model can be argued away, as done by Igi.[1] One simply assumes that in the resonance regions the slopes are not degenerate, but that at sufficiently large s all trajectories become parallel. No fundamental reason for this is offered, nor can one give the s range where the transition to a universal slope occurs. We will adopt this idea and employ it to discuss the decays of high-L $q\bar{q}$ states.

In a previous[2] article two of us examined the factorization properties of the leading Veneziano amplitude[4] for $PP \to PP$, [P a pseudoscalar in an SU(4) $\underline{15}+\underline{1}$ plet]. We found that nondegeneracy of slopes was related to the breakdown of nonet-type mass formulas for, e.g., ρ, D, and J [or SU(4) breaking of higher than first order]. Despite this, the parameters of the Regge trajectories were not arbitrary. We proposed equal-spacing rules for the trajectories. This and factorization of the trajectory slopes enabled us to express all slopes (at low s) in terms of one parameter. We then extracted the coupling constants of a meson of spin L (on the leading trajectory) to two pseudoscalars. The resulting predictions agree well with existing data. (These predictions hold for mesons L in the low-s range where the trajectories are nondegenerate but approximately linear).

In this article we extend the analysis to the case $VP \to PP$ where V is a vector meson lying on the leading trajectory. We show that a simple quark-line rule gives all LVP couplings in terms of only two parameters—an overall normalization and the slope of the ρ trajectory in the resonance region. Since we have nondegenerate slopes, SU(4) symmetry-breaking effects are included.

Section II is devoted to the derivation of our rule for LVP couplings. Decay widths are calculated in Sec. III, and our conclusions are in Sec. IV. Some details are left to Appendixes. Appendix A gives a derivation of the LVP coupling from $VP \to PP$ Veneziano amplitudes. Appendix B contains the decay rate formula for $L \to VP$ (L has natural parity and arbitrary spin).

II. LVP COUPLINGS

In this section we derive the LVP couplings from Veneziano's parametrization of the process[4]

$$V(\epsilon, k) + P_1(k_1) \to P_2(k_2) + P_3(k_3) \tag{2.1}$$

and study the asymptotic constraint on the Regge trajectory for this reaction (we are assuming that only asymptotically are trajectories linear and of the same slope for all reactions). The vector particle polarization is ϵ (momentum k) and the pseudoscalar momenta are k_1, k_2, k_3. The scattering amplitude is

$$T = \langle \epsilon k_1 k_2 k_3 \rangle t(s,t), \tag{2.2}$$

where $\langle abcd \rangle = \epsilon_{\mu\nu\lambda\sigma} a^\mu b^\nu c^\lambda d^\sigma$ and s, t, u are Mandelstam's variables. The vector meson is ρ, ω, ϕ, K^*, D^*, F^*, or J and the pseudoscalars are any threefold combination of π, K, D, F, and η_c, where η_c is the $c\bar{c}$ pseudoscalar (we will not discuss η and η' here, as they are not pure quark states). The amplitude $t(s,t)$ in (2.2) consists of one or more beta functions of the form

$$F_{AB}(s,t) = \frac{\Gamma(1-\alpha_A(s))\Gamma(1-\alpha_B(t))}{\Gamma(2-\alpha_A(s)-\alpha_B(t))}, \tag{2.3}$$

where $\alpha_A(s)$ and $\alpha_B(t)$ are the Regge trajectories contributing to the s and t channels. There are four sorts of amplitudes, depending on which external particles are present:

(1) Amplitudes crossing symmetric in all variables s, t, and u. This is Veneziano's original reaction $\omega\pi \to \pi\pi$. The amplitude $t(s,t,u)$ is

$$\lambda_1[F_{\rho\rho}(s,t) + F_{\rho\rho}(s,u) + F_{\rho\rho}(u,t)]. \tag{2.4}$$

(2) Amplitudes crossing symmetric in two variables (s and u, say) with all channels receiving contributions from definite Regge trajectories. This class contains

$$\omega K \to \pi K, \quad \omega D \to \pi D, \quad JD \to \eta_c D,$$
$$JF \to \eta_c F, \quad D^*\eta_c \to D\eta_c, \quad F^*\eta_c \to F\eta_c.$$

The amplitude involves two beta functions. The first four amplitudes are illustrated by $\omega K \to \pi K$, namely

$$\lambda_2[F_{K^*\rho}(s,t) + F_{K^*\rho}(u,t)], \tag{2.5}$$

and the last two are

$$\lambda_3[F_{D^*J}(s,t) - F_{D^*J}(u,t)]$$

and

$$\lambda_4[F_{F^*J}(s,t) - F_{F^*J}(u,t)]. \tag{2.6}$$

(3) Amplitudes with contributions from two channels (s and t, say) but with two exchange-degenerate trajectories (ρ-f and ω-A_2). The reactions involved are

$$K^*\bar{K} \to K\bar{K}, \quad K^*D \to KD,$$
$$D^*\bar{D} \to D\bar{D}, \quad F^*\bar{F} \to F\bar{F}.$$

In parametrizing these reactions, we separate the ρ-f contribution from the ω-A_2 contribution. For instance, $K^{*+}K^- \to K^+K^-$ is

$$\lambda_5[F_{\rho\phi}(s,t) + F_{\phi\rho}(s,t) + F_{\omega\phi}(s,t) + F_{\phi\omega}(s,t)]. \tag{2.7}$$

(4) Finally, amplitudes with two contributing channels (s and t, say), each with a unique Regge trajectory. There is only one term in the amplitude; as an example $\omega K \to \bar{D}F$ is given by

$$\lambda_6 F_{K^*D^*}(s,t). \tag{2.8}$$

In Eqs. (2.4)–(2.8), the λ's are normalization constants. Remarkably, there is only one independent constant. We now show how to reduce all the λ_i to multiples of a single λ.

In Appendix A we give the LVP couplings, g_V. As they stand, the couplings do not incorporate constraints relating them to one another. Two steps are necessary in order to do this:

(A) Consider four reactions with a fixed vector meson in the initial state. Each can be represented by a quark-line diagram where the two quarks in the vector meson are of fixed flavor. The others can be varied at will. The diagrams are shown in Fig. 1; q_1, q_2, ... q_4 label the quark lines with $q_1\bar{q}_3$

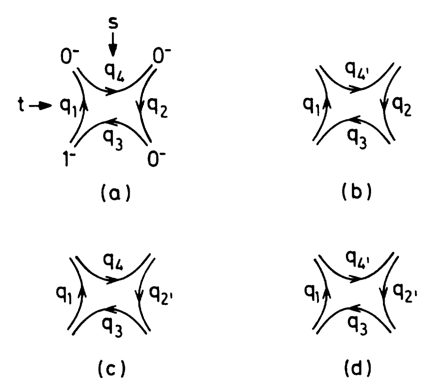

FIG. 1. Quark-line diagrams of two reactions $VP \to PP$ involving the same vector mesons but different pseudoscalar mesons. q_1, q_2, $\cdots$, and $q_{4'}$ label the quarks; $q_1\bar{q}_3$ is the vector-meson channel; the others are pseudoscalar-meson channels.

the vector-meson channel. Now notice that the same LVP coupling enters in the s channel of Figs. 1(a) and 1(b) and in Figs. 1(c) and 1(d). The same is true in the t channel of Figs. 1(a) and 1(c) and of Figs. 1(b) and 1(d). But since the same coupling enters in different reactions, all four must be related to one another. Then we find that the LVP couplings can be expressed in the following form:

$$\xi\lambda \frac{\alpha'_{22}}{\alpha'_{12}} (\alpha'_{33})^{L-1} N_L \,, \tag{2.9}$$

where $N_L^{-1} = 2^L(L-1)!$, λ is a common constant for a given vector meson, and ξ is an SU(4) Clebsch-Gordan coefficient. The slope parameters are those of the trajectories having the quantum numbers of $q_1\bar{q}_2$, $q_2\bar{q}_2$, $q_3\bar{q}_3$, where $q_1\bar{q}_2$ is the L channel, $q_1\bar{q}_3$ the vector-meson channel (held fixed) and $q_3\bar{q}_2$ the pseudoscalar channel.

We will illustrate this procedure by deriving the consistency condition for the s-channel couplings of Figs. 1(a) and 1(b). From Appendix A, Eq. (8), we have

$$a \frac{1}{\alpha'_{12}} \frac{(\alpha'_{34})^{2L-2}}{(\alpha'_{44})^{L}} N_L = a \frac{1}{\alpha'_{12}} \frac{(\alpha'_{33})^{L-1}}{\alpha'_{44}} N_L \,,$$

$$b \frac{1}{\alpha'_{12}} \frac{(\alpha'_{34})^{2L-2}}{(\alpha'_{4'4'})^{L}} N_L = b \frac{1}{\alpha'_{12}} \frac{(\alpha_{33})^{L-1}}{\alpha'_{4'4'}} N_L \,,$$

where we have used the factorization property of the slopes $\alpha'_{33}\alpha'_{44} = (\alpha'_{34})^2$, etc. Since the two couplings are identical we find

$$a/\alpha'_{44} = b/\alpha'_{4'4'} \,,$$

and we can choose $a = \lambda\alpha'_{44}$ and $b = \lambda\alpha'_{4'4'}$, delivering the promised relation between the normalization of Figs. 1(a) and 1(b). We can handle the normalizations of Figs. 1(c) and 1(d) the same way. Applying this procedure to the pairs 1(a)-1(c) and 1(b)-1(d), the normalization of all four reactions are fixed relative to one another and Eq. (2.9) follows. We have not assumed SU(4) symmetry for the couplings in this. The Clebsch-Gordan coefficients follow from the LPP couplings in our discussion of the LVP vertex in Appendix A, and by the crossing properties of $VP \to PP$. For degenerate Regge slopes both LPP couplings and LVP couplings are in fact SU(4) symmetric.

(B) Still another constraint has to be satisfied by the couplings. Two LVP couplings can be related by interchanging the quantum numbers of L and V. In the notation of Eq. (2.9) they are

$$\lambda_2 \frac{\alpha'_{22}}{\alpha'_{12}} (\alpha'_{33})^{L-1} N_L$$

and

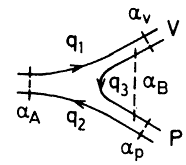

FIG. 2. Quark-diagram interpretation of the symmetry-breaking effect of Eq. (2.12); $q_1\bar{q}_3$ and $q_3\bar{q}_2$ are respectively the vector-meson and pseudoscalar-meson channels.

$$\lambda_3 \frac{\alpha'_{33}}{\alpha'_{13}} (\alpha'_{22})^{L-1} N_L \,.$$

Of course, for $L=1$ the L meson is a vector meson and the above two couplings are identical. Then

$$\lambda_2 \frac{\alpha'_{22}}{\alpha'_{12}} = \lambda_3 \frac{\alpha'_{33}}{\alpha'_{13}} \,. \tag{2.10}$$

If we use the factorization conditions $\alpha'_{12} = (\alpha'_{11}\alpha'_{22})^{1/2}$ and $\alpha'_{13} = (\alpha'_{11}\alpha'_{33})^{1/2}$, (2.10) can be satisfied in a symmetrical fashion by taking

$$\lambda_2 \equiv \lambda(\alpha'_{33}\alpha'_{11})^{1/2}, \quad \lambda_3 \equiv \lambda(\alpha'_{23}\alpha'_{11})^{1/2} \,.$$

Now we get the final form for the LVP couplings,

$$g_V{}^2 = g_{LVP}{}^2 = \xi\lambda\alpha'_{23}(\alpha'_{33})^{L-1} N_L \,, \tag{2.11}$$

where λ is just an overall normalization constant, common to all reactions.

Equation (2.11) is easily interpreted using the quark line diagram of Fig. 2. To show how symmetry breaking enters, write (2.11) as

$$g_V{}^2 = \xi\lambda \left(\frac{\alpha'_P}{\alpha'_\rho}\right) \left(\frac{\alpha'_B}{\alpha'_\rho}\right)^{L-1} (\alpha'_\rho)^{L-2} N_L \,, \tag{2.12}$$

where $\alpha'_P = \alpha'_{23}$ is the slope of the Regge trajectory with the quark content of the pseudoscalar in Fig. 2 and $\alpha'_B = \alpha'_{33}$ is the slope of the trajectory with the quark content of the pair created in the vertex of Fig. 2. We will discuss yet another form for (2.12) later.

III. DECAY RATES

In this section we present predictions for decay rates (including symmetry-breaking effects). In Sec. II we derive our main result for the LVP vertex (Eq. 2.12); the symmetry-breaking effects are contained in the factor

$$(\alpha'_P/\alpha'_\rho)(\alpha'_B/\alpha'_\rho)^{L-1} \,, \tag{3.1a}$$

which we can rewrite yet again (using the factorization property of the Regge slopes)

$$(\alpha'_\rho/\alpha'_A)(\alpha'_V/\alpha'_\rho)(\alpha'_P/\alpha'_\rho)^2(\alpha'_B/\alpha'_\rho)^{L-2} \,. \tag{3.1b}$$

α'_V is the vector-meson trajectory slope, and α'_A is that of the decaying meson L. Notice that α'_B

$=\alpha'_\rho$, α'_ϕ, or α'_J, depending on the flavor of the created quark pair in the vertex of Fig. 2. The factor $(\alpha'_B/\alpha'_\rho)^{L-2}$ clearly disfavors the creation of a heavy-quark pair in Fig. 2, inasmuch as $\alpha'_B < \alpha'_\rho$. The factor $1/\alpha'_A$ always appears in the decay amplitude for a particle lying on a Regge trajectory of slope α'_A.[5]

It is instructive to compare the LVP (g_V) and the LPP couplings (g_P) derived in Ref. (2) and given in the Appendix (Eq. A7). We find

$$g_P{}^2=\lambda_0\left(\frac{\alpha'_\rho}{\alpha'_A}\right)\left(\frac{\alpha'_B}{\alpha'_\rho}\right)^L(\alpha'_\rho)^L N_L\,.$$

Because of the different spin structure of the coupling, no dependence on α'_V and α'_P is present [see Eq. (3.1b)].

Substituting (2.12) into the decay rate expression (Eq. B4) we have

$$\Gamma_{L\to VP}=\frac{\xi\lambda}{4\pi}\frac{\alpha'_P}{\alpha'_\rho}\left(\frac{\alpha'_B}{\alpha'_\rho}\right)^{L-1}(\alpha'_\rho)^{L-2}\times\frac{1}{2L+1}\frac{2^{2L-3}(L+1)!}{(2L)!}k^{2L+1}\,, \qquad (3.2)$$

where k is the c.m. momentum of V or P in the decay. The ratios of slopes from Ref. 2 are $\alpha'_{K^*}/\alpha'_\rho=0.924$, $\alpha'_\phi/\alpha'_\rho=0.854$, $\alpha'_{D^*}/\alpha'_\rho=0.761$, $\alpha'_{F^*}/\alpha'_\rho=0.703$, and $\alpha'_J/\alpha'_\rho=0.579$. As in Ref. 2 we use $\alpha'_\rho=0.88\ \mathrm{GeV}^{-2}$. Then all rates are fixed by one parameter λ. We use the rate for $A_2\to\rho\pi$ (Ref. 6) (which is the most accurate) to get

$$\lambda/4\pi=15.4\ \mathrm{GeV}^{-4},$$

with $\xi=4$. In Table I we list the calculated decay rates for the low-spin mesons together with available experimental values. The ξ coefficients (relative to that for $A_2\rho\pi$) are also listed.

TABLE I. Partial decay rates. $\bar{\xi}$ is obtained from ξ by combining different isospin channels. The mass values used for D^{**}, etc. are derived in Ref. 2, $m_{D^{**}}=2.35$, $m_{F^{**}}=2.49$, $m_{D^{***}}=2.65$, $m_{F^{***}}=2.80$ GeV. Their partial widths are just sample calculations to show the order of magnitude. The decays $F^{**}\to D^*K$, $D^{***}\to\omega D$, $F^{***}\to K^*D$, etc. are either below the threshold, or very close to the threshold. We do not attempt to calculate them.

	$\bar{\xi}$	Theory (MeV)	Exp. (MeV)
		Tensor meson $J^P=2^+$ decays	
$A_2\to\rho\pi$	4		72.3 ± 4.0
$K^{**}\to K^*\pi$	$\frac{3}{2}$	28.5 ± 1.7	33.4 ± 3.8
$\to\rho K$	$\frac{3}{2}$	6.7 ± 0.4	7.1 ± 2.0
$\to\omega K$	$\frac{1}{2}$	1.9 ± 0.1	4.9 ± 1.9
$f'\to K^*\bar{K}+\bar{K}^*K$	4	12.1 ± 0.8	
$D^{**}\to D^*\pi$	$\frac{3}{2}$	4.6	
		$J^P=3^-$ decays	
$g\to\omega\pi$	2	53.4 ± 32	large 4π mode
$\to K^*\bar{K}+\bar{K}^*K$	2	3.4 ± 0.2	small
ω (1675) $\to\rho\pi$	6	148.3 ± 8.7	seen
$\to K^*\bar{K}+\bar{K}^*K$	2	2.6 ± 0.2	
K_N (1800) $\to K^*\pi$	$\frac{3}{2}$	46.7 ± 2.8	
$\to\rho K$	$\frac{3}{2}$	29.3 ± 1.8	
$\to\omega K$	$\frac{1}{2}$	8.9 ± 0.5	
$\to\phi K$	1	1.6	
$D^{***}\to D^*\pi$	$\frac{3}{2}$	11.7	
$F^{***}\to D^*K$	2	8.3	

IV. CONCLUSION

Our main result is that for L, a meson of not too high spin on a leading Regge trajectory, LVP couplings can be read off a quark-line diagram (Fig. 2). Symmetry breaking enters through nondegenerate slopes for certain $q\bar{q}$ trajectories. We have given rates for decays of L to a vector plus pseudoscalar meson. Large symmetry-breaking effects occur in the couplings of nonstrange and uncharmed mesons L into strange and/or charmed particles. Except when the final state involves η_c or F or requires that an $s\bar{s}$ or $c\bar{c}$ pair be created from the vacuum, we find little suppression of charmed-meson decays due to symmetry breaking.

We close with some specific remarks:

(1) Our rate predictions compare well with the (scanty) data. We remark that from $A_2\to\rho\pi$ we predict that $\omega(1695)$ [which has a width of 150 $\pm$ 20 MeV (Ref. 6)] decays principally to $\rho\pi$ (148 MeV). A measurement of this decay would be welcome.

(2) Our predicted $K^{**}\to\omega K$ width is about $1\frac{1}{2}$ standard deviations away from the experimental result (which has a rather large error, see Table I). An accurate measurement of this width checks this and any other model relating $A_2\to\rho\pi$ and $K^{**}\to\omega K$ and incorporating SU(3) breaking.

(3) From its $K\pi$ and $K^*\pi$, ρK modes, we predict that $K_N(1800)$ has a width $\gtrsim$120 MeV.

(4) Since charmed-meson decay rates are little affected by symmetry breaking, the real tests of the scheme lie in the relations between $L\to PP$ and $L\to VP$ rates.

We believe that Veneziano amplitudes with nondegenerate trajectories offer a useful phenomenological description of the decays of moderately-high-L $q\bar{q}$ states on leading Regge trajectories. This contrasts with the nonrelativistic quark model, which we believe better suited to describe states of low L.[7]

ACKNOWLEDGMENTS

The work of M.K. was supported by the Alexander von Humboldt Foundation. The work of B.-L.Y. was supported in part by ERDA under Contract No. W-7405-Eng-82.

APPENDIX A: THE LVP COUPLING

Let the reaction (2.1) be described by a one-term Veneziano amplitude (the generalization to more than one term is straightforward):

$$t(s,t)=\lambda F_{AB}(s,t)=\lambda\,\frac{\Gamma(1-\alpha_A(s))\Gamma(1-\alpha_B(t))}{\Gamma(2-\alpha_A(s)-\alpha_B(t))}\,. \tag{A1}$$

The resonance L of mass m_L and spin L contributes to the s channel. The contribution of L to T is

$$T\to\frac{1}{s-m_L^{\,2}}\sum_\eta[g_P h_{\mu_1\cdots\mu_L}(\eta)\Delta_f^{\mu_1}\cdots\Delta_f^{\mu_L}][g_V h_{\nu_1\cdots\nu_L}(\eta)\Delta_i^{\nu_1}\cdots\Delta_i^{\nu_L}]\langle\nu_1\epsilon k k_1\rangle\,, \tag{A2}$$

where $\Delta_f=k_2-k_3$, $\Delta_i=k-k_1$, $h_{\mu_1\cdots\mu_L}(\eta)$ is the polarization state η. The terms in the first and second set of brackets of (A2) are the LPP coupling (g_P) and the LVP coupling (g_V). Now we use

$$\sum_\eta h_{\mu_1\cdots\mu_L}(\eta)h^*_{\nu_1\cdots\nu_L}(\eta)=\frac{1}{L!}(-)^L\sum_{\substack{j_1\cdots j_L\\ \text{permutations}\\ \nu_1\cdots\nu_L}} g_{\mu_1\nu_{j_1}}\cdots g_{\mu_L\nu_{j_L}} \tag{A3}$$
$$+\text{terms proportional to } K=k_1+k=k_2+k_3$$

and note that from the helicity amplitude that $T\propto\sin\theta P_L'(\cos\theta)$ ($\sin\theta$ comes from $\langle\epsilon k_1k_2k_3\rangle$ and P_L' is the first derivative of the Lth Legendre polynomial). Only the first term in (A3) contributes to the highest power of $\cos\theta$ $(\cos\theta)^{L-1}$ and we can thus read off the coefficient of $\mathcal{P}_L'$,

$$T\to\langle\epsilon k_1k_2k_3\rangle\left(-(4k_ik_f)^{L-1}g_Vg_P\,\frac{2^{L+1}(L!)^2}{L(2L)!}\right)P_L'(\cos\theta)\,\frac{1}{s-m_L^{\,2}}\,, \tag{A4}$$

where k_i and k_f are initial and final c.m. momenta. Doing the same thing for the Veneziano amplitude we find for $s \to m_L^2$, $\alpha_A(s) \to L$,

$$T \to \langle \epsilon k_1 k_2 k_3 \rangle \left(-\frac{\lambda_1}{\alpha'_A} (4k_i k_f)^{L-1} (\alpha'_B)^{L-1} \frac{2(L!)}{(2L)!} \right) P'_L(\cos\theta) \frac{1}{s - m_L^2} . \tag{A5}$$

Comparing (A4) and (A5) we have

$$g_V g_P = \frac{\lambda_1}{\alpha'_A} (\alpha'_B)^{L-1} N_L, \quad N_L = \frac{1}{2^L (L-1)!} , \tag{A6}$$

where, from Ref. 2

$$g_P^2 = \frac{\lambda_0}{\alpha'_A} (\alpha'_{B'})^{L-1} N_L \tag{A7}$$

$(\alpha'_{B'})$ is in general different from α'_B). Equation (A7) has a quark-diagram interpretation: If L is composed of $q_1\bar{q}_2$ the two pseudoscalars are $q_1\bar{q}_3$ and $q_3\bar{q}_2$ with $\alpha'_{B'} = \alpha_{q_3\bar{q}_3}$. From (A6) and (A7) we extract our final result,

$$g_V^2 = \frac{\lambda}{\alpha'_A} \frac{(\alpha'_B)^{2L-2}}{(\alpha'_{B'})^L} N_L , \tag{A8}$$

where $\lambda = \lambda_1^2/\lambda_0$.

APPENDIX B: DECAY RATES

The derivation uses the unitarity relation for $V(k_a, \epsilon_i) + P(k_b) \to V(k_c, \epsilon_f) + P(k_d)$. Polarization vectors and momenta are as indicated. Our coordinates are

$$\begin{aligned} &k_a = (E_a, 0, 0, k), \quad k_b = (E_b, 0, 0, -k) , \\ &k_c = (E_a, k \sin\theta, 0, k\cos\theta) , \quad k_d = (E_b, -k\sin\theta, 0, -k\cos\theta) , \\ &\epsilon_i(\pm) = \frac{1}{\sqrt{2}} (0, \pm 1, -i, 0), \quad \epsilon_f^*(\pm) = \frac{1}{\sqrt{2}} (0, \mp\cos\theta, \pm i, \pm\sin\theta) . \end{aligned} \tag{B1}$$

For a natural-parity meson L coupling to VP, the only independent helicity amplitude is easily seen to be $T_{11} = T_{-1-1}$ $(T_{00} = 0)$. Labeling initial and final helicities of the vector meson by η_i, η_f we have as $s \to m_L^2$,

$$T_{\eta_f \eta_i} \to \frac{g_V^2}{s - m_L^2} \sum_{\eta} [h_{\nu_1 \cdots \nu_L}(\eta) \Delta_f^{\nu_2} \cdots \Delta_f^{\nu_L} \langle \nu_1 \epsilon_f^*(\eta_f) k_c k_d \rangle] [h_{\mu_1 \cdots \mu_1}(\eta) \Delta_f^{\mu_2} \cdots \Delta_f^{\mu_2} \langle \mu_1 \epsilon(\eta_1) k_a k_b \rangle] , \tag{B2}$$

where $k_i = k_a - k_b$, $k_f = k_c - k_d$. As in Appendix A we extract the highest power of $\cos\theta$ and find

$$T_{11} \to g_V^2 m_L^2 k^{2L} \frac{2^{3L-3}(L+1)!\,(L-1)!}{(2L)!} \frac{d_{11}^L(\theta)}{s - m_L^2} , \tag{B3}$$

and the decay rate is given by

$$\Gamma_{L\to VP} = \frac{k}{8\pi m_L^2} \lim_{s\to m_L^2} \int_{-1}^{1} d\cos\theta \, T_{11}^L d_{11}^L(\theta) = \frac{g_V^2}{4\pi} \frac{1}{2L+1} \left(\frac{2^{3L-3}(L-1)!\,(L+1)!}{(2L)!} \right) k^{2L+1} . \tag{B4}$$

---

*Permanent address.

[1]K. Igi, Phys. Rev. D 15, 865 (1977); Phys. Lett. 66B, 276 (1977).

[2]Masaaki Kuroda and Bing-Lin Young, Phys. Rev. D 16, 204 (1977).

[3]S. Mandelstam, Phys. Rev. Lett. 21, 1724 (1968).

[4]G. Veneziano, Nuovo Cimento 57A, 190 (1968).

[5]See for example, S. C. Frautschi, *Regge Poles and S-Matrix Theory* (Benjamin, New York, 1963).

[6]Particle Data Group, Rev. Mod. Phys. 48, S1 (1976).

[7]See, however, the relativistic quark-model calculations of M. Böhm, H. Joos, and M. Krammer, CERN Report No. CERN TH 1949, 1974 (unpublished).

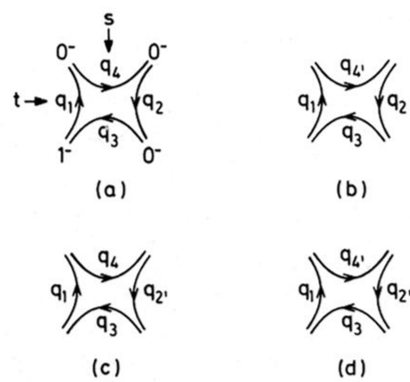

FIG. 1. Quark-line diagrams of two reactions $VP \to PP$ involving the same vector mesons but different pseudoscalar mesons. q_1, q_2, $\cdots$, and $q_{4'}$ label the quarks; $q_1 \bar{q}_3$ is the vector-meson channel; the others are pseudoscalar-meson channels.

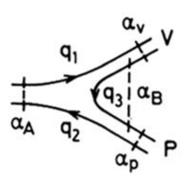

FIG. 2. Quark-diagram interpretation of the symmetry-breaking effect of Eq. (2.12); $q_1\bar{q}_3$ and $q_3\bar{q}_2$ are respectively the vector-meson and pseudoscalar-meson channels.